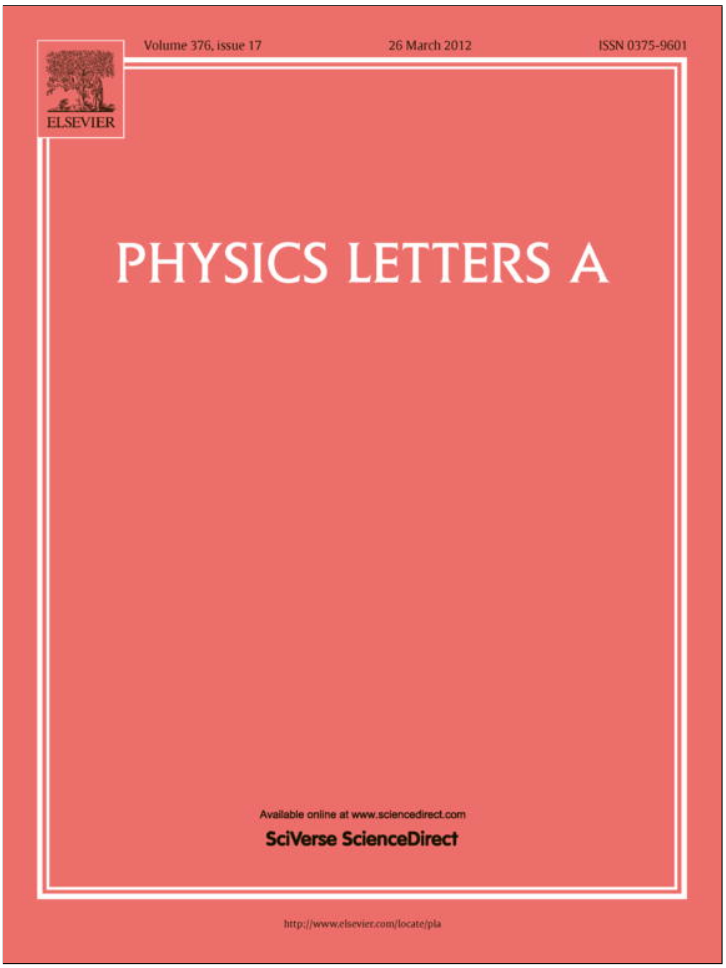

Physics Letters A 376 (2012) 1509–1514

Contents lists available at SciVerse ScienceDirect

Physics Letters A

www.elsevier.com/locate/pla

Suppression of Anderson localization in a graphene sheet applied by a random voltage pattern

Hai-tao Jiang *, Jie-fei Zhang, Zi-li Wang, Yun-hui Li, Hong Chen

Key Laboratory of Advanced Microstructure Materials, MOE, Department of Physics, Tongji University, Shanghai 200092, China

ARTICLE INFO

Article history:
Received 28 October 2011
Received in revised form 9 March 2012
Accepted 10 March 2012
Available online 13 March 2012
Communicated by V.M. Agranovich

Keywords:
Graphene
Anderson localization
Phase compensation

ABSTRACT

We theoretically study the transport of electronic waves through a graphene sheet applied by a random voltage pattern in which the magnitudes and/or the widths of the voltages are random. When the magnitudes of the voltages exceed the electronic energy, the applied region can be considered as left-handed (LH) layers. Compared to the disordered structures with right-handed (RH) layers only, the spectra of the (average) density of states and the localization lengths in mixed random structures with RH and LH layers all show the suppression of Anderson localization, owing to the phase compensation effect of LH layers that reduces the long-range interference in the random system.

1. Introduction

Anderson localization, one of the most fundamental and intriguing phenomena in random systems, describes the behavior of particles in a maze. After the concept of Anderson localization was originally conceived from the absence of spin or electronic diffusion in disordered lattices [1], Anderson localization has been found widely exist for other one-particle excitations and classical waves [2–5]. Anderson localization comes from the interferences of multiply scattered waves in a random structure. Although random scattering is naturally a three-dimensional problem, one-dimensional (1D) sufficiently long, random structures still attract people's attention in that they can capture the main characteristics of Anderson localization [2,5]. In an infinite 1D disordered system, the main indication of localization is the exponential decay of the amplitude of a wave inside the structure. The rate of this decay is called the Lyapunov exponent, γ, the inverse value of which determines the spatial size of localization [2]. In a long, finite sample, the localization is manifested by the exponential decay of the transmission coefficient. The characteristic length of this decay is termed the transmission length l_T. When the sample size tends to infinite, l_T becomes the localization length l which, in general, coincides with the inverse of Lyapunov exponent γ^{-1}. In the localized regime, where l_T is much smaller than the sample length, l_T is generally in accordance with l.

Recently, random structures with left-handed (LH) metamaterials make Anderson localization for classical waves more interesting and intriguing. In LH metamaterials, the electric field vector, the magnetic field vector, and the wave vector form a LH rule instead of the right-handed (RH) rule in normal materials [6]. As a result, the directions of the wave vector (or phase velocity) and the energy flow (or group velocity) are antiparallel, which leads to many unusual phenomena such as negative refraction [7], zero-averaged refractive-index gaps [8], etc. In particular, A.A. Asatryan et al. systematically studied the properties of 1D mixed disordered stack of alternating RH and LH layers [9–11]. They found that, owing to the phase compensation effect of LH metamaterials, Anderson localization could be noticeably suppressed. An example of the suppression is that, in the long-wave region where the interference is weak, the localization length in mixed stacks obeys the $l \propto \lambda^6$ (where λ is the wave length) law [9] rather than the universal $l \propto \lambda^2$ one for normal random stacks with pure RH layers [12]. A more real model using dispersive LH metamaterials further confirmed the suppression of Anderson localization [13]. Non-localized modes and the abnormal finite-size scaling law were also found in mixed disordered stacks [14,15]. Up to now, all the suppressions of Anderson localization are predicted for classical waves. A natural question to ask is can we go back to the electronic systems where the concept of Anderson localization is conceived and find the suppressions of Anderson localization in the random electronic systems?

The answer becomes positive, with the rapid emergency of a new electronic medium named graphene that is a monolayer of carbon atoms arranged in a honeycomb pattern [16]. The special

* Corresponding author.
E-mail address: jiang-haitao@tongji.edu.cn (H.-t. Jiang).

0375-9601/$ – see front matter
http://dx.doi.org/10.1016/j.physleta.2012.03.026

topology structure of graphene ensures that graphene has Dirac cone energy dispersion and many other unusual properties [17,18]. In particular, a graphene sheet applied by suitable external voltages can become a LH electronic medium in which the direction of the wave vector of an electron is opposite to that of the group velocity. When a LH graphene medium is combined with a RH graphene medium, the electron flow can be negatively refracted at the interface of the two media [19], in analogy with the negative refraction of light [7]. Moreover, the phase compensation effect of LH electronic medium in the composite structure can modify the transport properties of electrons greatly. For example, in a superlattice composed of alternating RH and LH graphene medium, a zero-averaged wave number gap that is distinct from a Bragg gap can appear [20]. Also, backward electronic Tamm states can occur in a heterostructure containing LH graphene medium [21]. In this Letter, we extend the phase compensation effect to the random electronic systems with LH graphene media. By applying a random voltage pattern, in which the magnitudes and/or the widths of the voltages are random, on a graphene sheet, we calculate the (average) density of states and the localization length as a function of energy at different disorder degrees. We find that the Anderson localization is noticeably suppressed, owing to the phase compensation effect of LH graphene media. The suppression of Anderson localization in electronic counterparts may extend our understanding of the behavior of particles in complex random quantum systems.

2. Suppression of Anderson localization

If an external voltage $V(x)$ that varies with the coordinate x is applied on a graphene sheet, the Hamiltonian of an electron inside can be written as

$$\hat{H} = \upsilon_F \boldsymbol{\sigma} \bullet \mathbf{p} + V(x)\hat{I}, \tag{1}$$

where $\upsilon_F \approx 10^6$ m/s is the Fermi velocity, $\boldsymbol{\sigma} = (\sigma_x, \sigma_y)$ with σ_x, σ_y being Pauli matrices of the pseudospin, $\mathbf{p} = (-i\hbar\frac{\partial}{\partial x}, -i\hbar\frac{\partial}{\partial y})$ is the momentum operator, and $\hat{I}$ is a 2×2 unit matrix. The two non-degenerated wave functions acted by $\hat{H}$ are written as $\boldsymbol{\psi} = (\tilde{\psi}_A, \tilde{\psi}_B)^T$, where $\tilde{\psi}_{A,B}(x,y) = \psi_{A,B}(x)e^{i\beta y}$. β is the component of the wave vector along y coordinate and depends on the angle of incidence θ_0. From the equation $\hat{H}\boldsymbol{\psi} = E\boldsymbol{\psi}$, where E is the energy of an incident electron, one can obtain the following wave equations describing the transport of an electron inside a graphene sheet applied by $V(x)$:

$$\frac{d\psi_A}{dx} - \beta\psi_A = ik\psi_B, \tag{2}$$

$$\frac{d\psi_B}{dx} + \beta\psi_B = ik\psi_A, \tag{3}$$

where $k = [E - V(x)]/\hbar\upsilon_F$ is the wave vector of the electron inside the graphene. In particular, if $E < V(x)$, the direction of k inside the potential will be antiparallel with that of group velocity and the corresponding region becomes a LH electronic medium. In what follows, by controlling the magnitudes of voltages applied on the graphene, some layers, in which the potentials exceed the electronic energy, can be used as LH media.

A 1D graphene sheet applied with a random voltage profile is schematically shown in Fig. 1. The white and gray layers in the graphene sheet are denoted by A and B applied with potentials V_A and V_B, respectively. The thicknesses of A and B are represented by d_A and d_B, respectively. The magnitudes of the applied voltages can be arbitrary. The thickness of each layer, i.e., the width of each voltage in x direction, can also be random. Once the values of V_{Aj}, V_{Bj}, d_{Aj} and d_{Bj} of the arbitrary jth layer are given, the complex transmission coefficient $t = |t|\exp(i\Phi)$, where Φ is the total phase accumulated by the electron propagating through the graphene sheet, can be calculated by means of the transfer-matrix method [20,21]. Then, the effective wave vector can be derived by $K_{eff} = \Phi/L$, where L is the total width of the sheet. In analogy with the definition for the density of photonic states in a 1D dielectric structure [22,23], the density of electronic states in our structure can be obtained by $\rho(E) = \mathrm{d}K_{eff}/\mathrm{d}E$. We consider three cases: (i) only the magnitudes of voltages are random, (ii) only the widths of voltages are random and (iii) both the magnitudes and the widths of voltages are random. An $(AB)_{30}$ structure with 30 A and 30 B layers is considered and the angle of incidence θ_0 is assumed to be 15 degrees in three cases.

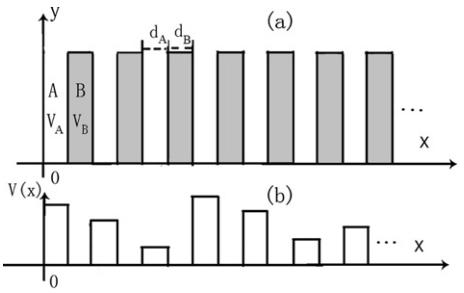

Fig. 1. (a) Schematic of a graphene sheet structure. The white and gray layers are denoted by A and B that are applied with electrostatic potentials V_A and V_B, respectively. The thicknesses of A and B are represented by d_A and d_B, respectively. (b) The profile of the potentials applied on the graphene sheet.

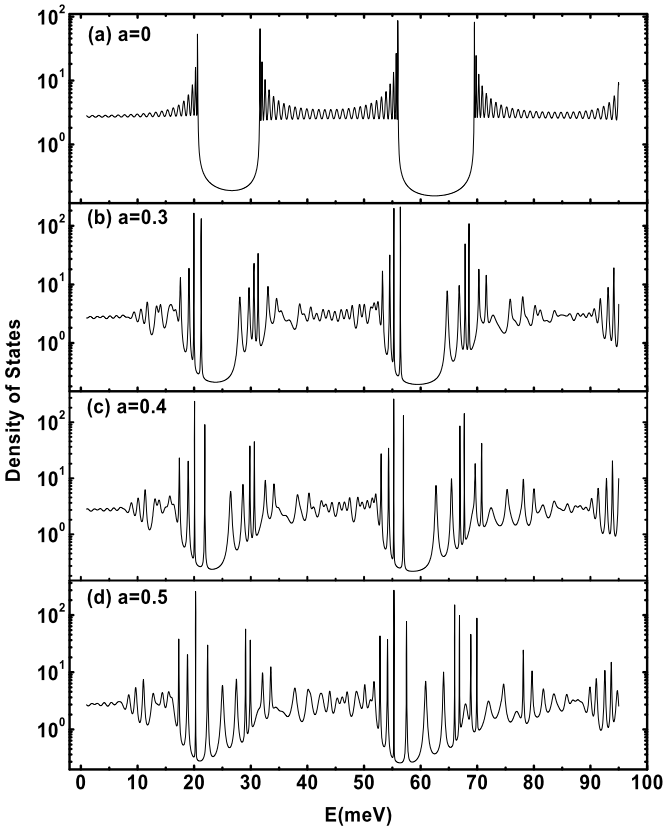

Fig. 2. The spectra of density of states for $(AB)_{30}$ structures with a given configuration of random voltage-magnitude for (a) $a = 0$, (b) $a = 0.3$, (c) $a = 0.4$ and (d) $a = 0.5$, respectively, where subscript 30 is the number of layer A or B. $\theta_0 = 15°$, $d_A = d_B = 30$ nm, $V_{Aj} = 50(1 + a*\delta)$, $V_{Bj} = a*\delta$ meV ($j = 1, 2, 3, \ldots, 30$).

Now we calculate the spectra of density of states (DOS) for a structure with a fixed random configuration in each case. At first, we apply a voltage pattern, in which only the magnitudes are random, on the sheet to see the influence of the phase com-

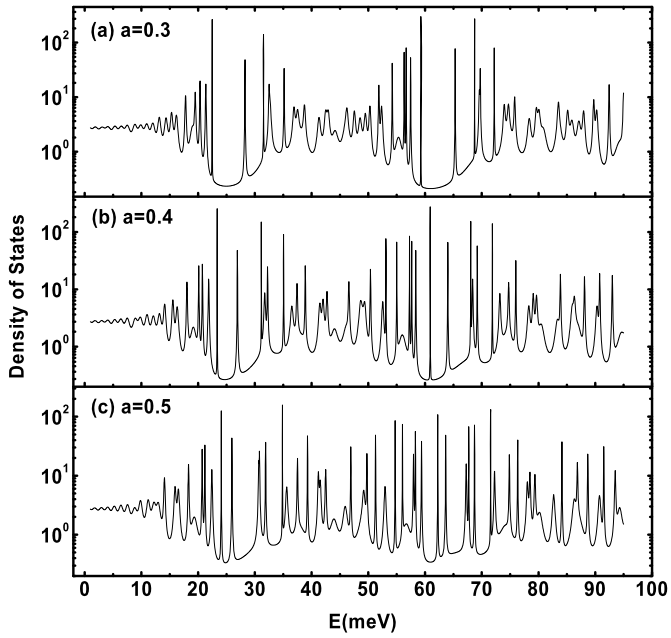

Fig. 3. The spectra of density of states for $(AB)_{30}$ structures with a given configuration of random thickness for (a) $a = 0.3$, (b) $a = 0.4$ and (c) $a = 0.5$, respectively. $\theta_0 = 15°$, $V_A = 50$ meV, $V_B = 0$, $d_{Aj} = 30(1 + a * \delta)$ nm, $d_{Bj} = 60 - d_{Aj}$ nm ($j = 1, 2, 3, \ldots, 30$).

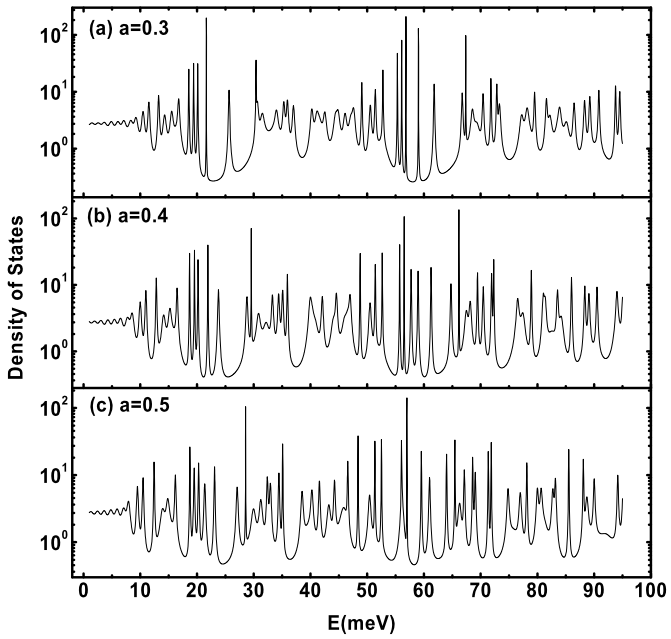

Fig. 4. The spectra of density of states for $(AB)_{30}$ structures with a given configuration of random voltage-magnitude and thickness for (a) $a = 0.3$, (b) $a = 0.4$ and (c) $a = 0.5$, respectively. $\theta_0 = 15°$, $V_{Aj} = 50(1 + a * \delta)$ meV, $V_{Bj} = a * \delta$ meV, $d_{Aj} = 30(1 + a * \delta)$ nm, $d_{Bj} = 60 - d_{Aj}$ nm ($j = 1, 2, 3, \ldots, 30$).

pensation effect on Anderson localization. In practice, the voltage of each layer is much easier to tune than the refractive index of each layer for classical waves [9]. The thickness of A or B layer is fixed ($d_A = d_B = 30$ nm). The voltage-magnitudes of the jth A and B layers are assumed to be $V_{Aj} = 50(1 + a * \delta)$ meV and $V_{Bj} = a * \delta$ meV, respectively, where a ($0 \leqslant a < 1$) describes the degree of disorder and δ are independent random variables distributed uniformly on $[-1, 1]$. Here we point out that the definitions of a and δ are same throughout the Letter. In Fig. 2 we show the variances of the spectra of DOS when the value of a

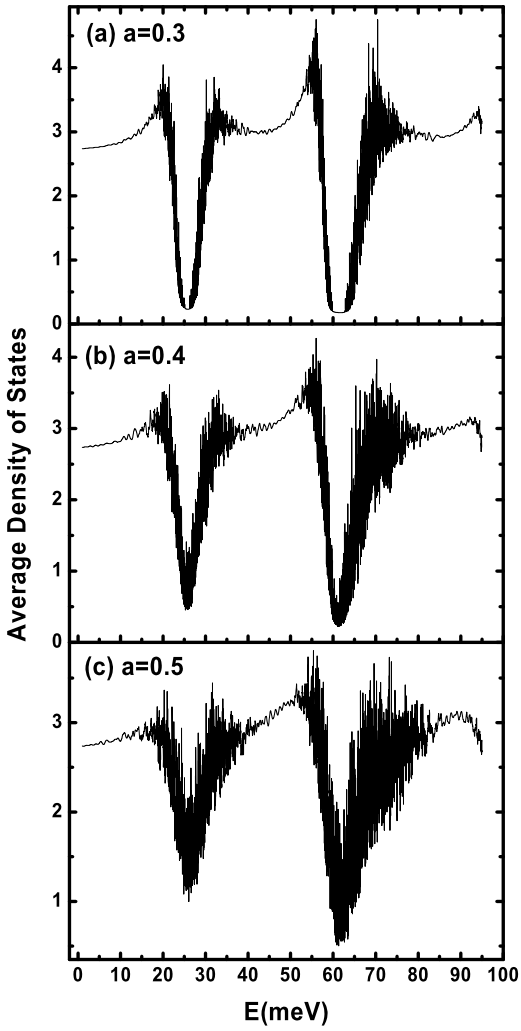

Fig. 5. The spectra of average density of states for $(AB)_{30}$ structures over 1000 configurations of random voltage-magnitude for (a) $a = 0.3$, (b) $a = 0.4$ and (c) $a = 0.5$, respectively. All the other parameters are the same with those used in Fig. 2.

increases from 0 to 0.5. The structure in which $a = 0$ is actually a periodic structure. When the electronic energy is less than the voltage-magnitude of the jth A layer ($E < 50$ meV), the wave number in the A layer is negative and the A layer is a LH layer, while $E > 50$ meV, the A layer is a RH layer. Since no voltage is applied on the B layer, it is a RH layer in whole spectra. As a result, the lower DOS gap (about $20 < E < 30$ meV) in Fig. 2(a) is the zero-averaged wave number ($\langle k \rangle = k_A d_A + k_B d_B = 0$) gap [20] while the upper one (about $55 < E < 70$ meV) is a conventional Bragg gap. When the value of a increases from 0.3 to 0.5, the B layer is always a RH layer except that in a very small region in which the energy is near zero. Whether the A layer is a LH or RH one depends on the difference between the voltage-magnitude and the energy. If the voltage-magnitude is greater (smaller) than the energy, the A layer will be a LH (RH) one. With the increase of a, one can see that more and more discrete localized states induced by the voltage-magnitude disorder appear, as is shown in Figs. 2(b)–(d). However, the changing degree for extended states in the band with $0 < E < 20$ meV and those in the band with $75 < E < 95$ meV are quite different. The extended states in the band with $0 < E < 20$ meV are robust against a. When the value of a increases to 0.5, at $0 < E < 10$ meV only a few extended states become localized states. In contrast, the extended states in the band with $75 < E < 95$ meV are sensitive to a. When the value

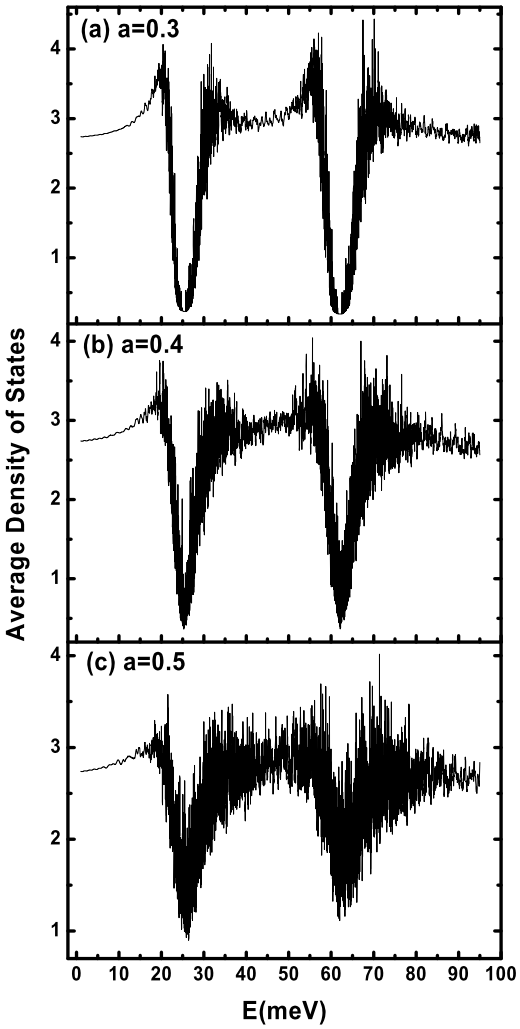

Fig. 6. The spectra of average density of states for $(AB)_{30}$ structures over 1000 configurations of random thickness for (a) $a = 0.3$, (b) $a = 0.4$ and (c) $a = 0.5$, respectively. All the other parameters are the same with those used in Fig. 3.

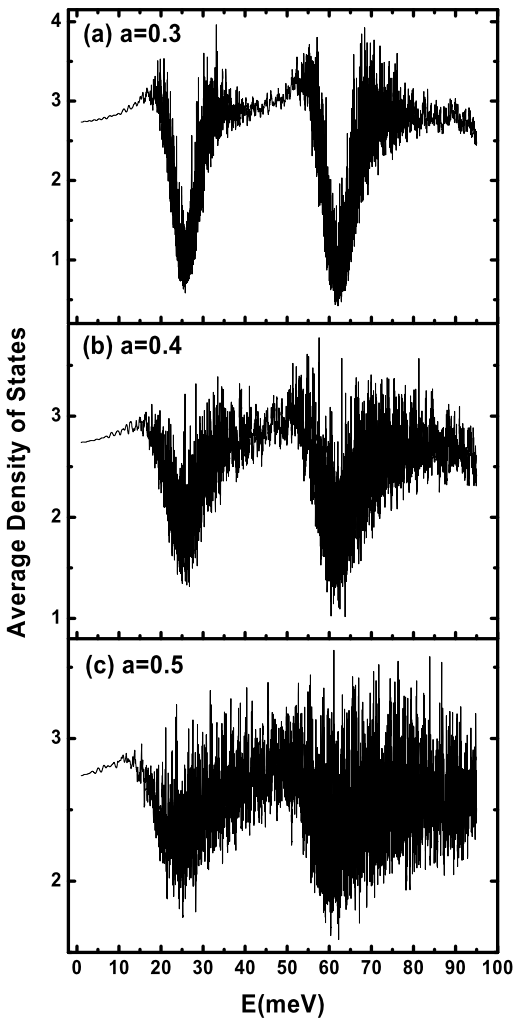

Fig. 7. The spectra of average density of states for $(AB)_{30}$ structures over 1000 configurations of random voltage-magnitude and thickness for (a) $a = 0.3$, (b) $a = 0.4$ and (c) $a = 0.5$, respectively. All the other parameters are the same with those used in Fig. 4.

of a increases to 0.5, almost all extended states become localized states. The physical reason is as follows. Under above parameters, in the band with $75 < E < 95$ meV, the A layer is also a RH layer. This means in this band the structure is a normal random structure with pure RH layers and the extended states are easy to evolve into the localized states as the disorder increases. However, in the band with $0 < E < 20$ meV, the A layer is always a LH layer. The phase compensation effect caused by the LH layer strongly reduces the long-range interferences and suppresses Anderson localization in the random structure. Next, we study the case in which only the widths of voltages are random. The magnitudes of applied voltages in A and B layers are fixed to be 50 meV and 0, respectively. To keep the total length of the $(AB)_{30}$ structure invariant, the thickness of each layer is assumed to be $d_{Aj} = 30(1 + a * \delta)$ nm and $d_{Bj} = 60 - d_{Aj}$ nm ($j = 1, 2, 3, \ldots, 30$). In Fig. 3 we show the variances of the spectra of the DOS when the value of a increases from 0.3 to 0.5. Since the voltage-magnitudes of A and B layers do not fluctuate, the A layer is always a LH layer when $E < 50$ meV and the B layer is always a RH one. From Fig. 3 one can see that the essential property, i.e., the changing degree from extended states to localized states in the mixed structure with LH layers ($E < 20$ meV) are slower than those in the structure with pure RH layers ($E > 75$ meV), still exists. This is because the phase compensation effect of the LH layers suppresses the Anderson localization induced by the thickness fluctuation. Finally we study the case in which both the magnitudes and the widths of voltages are random. Once again, an $(AB)_{30}$ structure, in which $V_{Aj} = 50(1 + a * \delta)$ meV, $V_{Bj} = a * \delta$ meV, $d_{Aj} = 30(1 + a * \delta)$ nm and $d_{Bj} = 60 - d_{Aj}$ nm ($j = 1, 2, 3, \ldots, 30$), is considered. In Fig. 4 we show the variances of the spectra of DOS when the value of a increases from 0.3 to 0.5. Comparing Fig. 4 with Fig. 2 and Fig. 3, one can see that the voltage-magnitude fluctuation together with the thickness fluctuation strengthens the evolution from extended states to localized states. However, the phase compensation effect of the LH layers to reduce Anderson localization still works.

In Figs. 2–4 we only show the behavior for a given disorder realization. To better illustrate the suppression of Anderson localization, we calculate the average DOS ($\langle \rho(E) \rangle$) obtained by ensemble averaging over 1000 configurations. Following the same turn in Figs. 2–4, in Figs. 5–7 we show the spectra of average DOS in three cases one by one. From Figs. 5–7 one can see that the sharp resonances in Figs. 2–4 are strongly destroyed by the disorder averaging. However, some properties displayed in Figs. 2–4 are still maintained in Figs. 5–7. For example, the tendency towards localization, e.g., the smearing of the energy gaps, is strengthened as the degree of disorder increases. Besides, the tendency in the case involving both voltage-magnitude and thickness fluctuations is most obvious. Moreover, the extended states in the mixed struc-

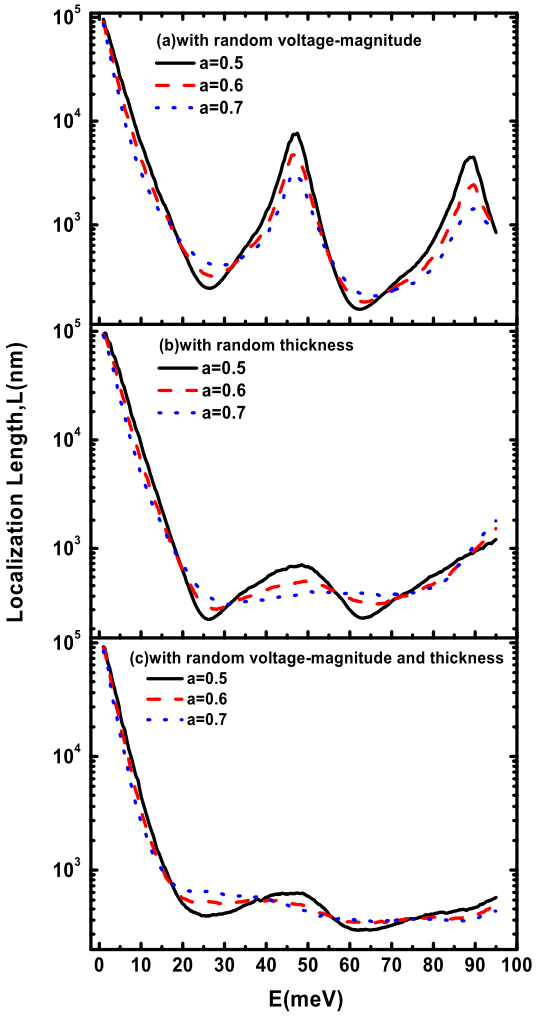

Fig. 8. The spectra of localization lengths of $(AB)_{30}$ structures over 1000 configurations of (a) random voltage-magnitude, (b) random thickness, (c) random voltage-magnitude and thickness, respectively. The corresponding parameters are the same with those used in Figs. 2–4. The solid line: $a = 0.5$; the dashed line: $a = 0.6$; the dotted line: $a = 0.7$.

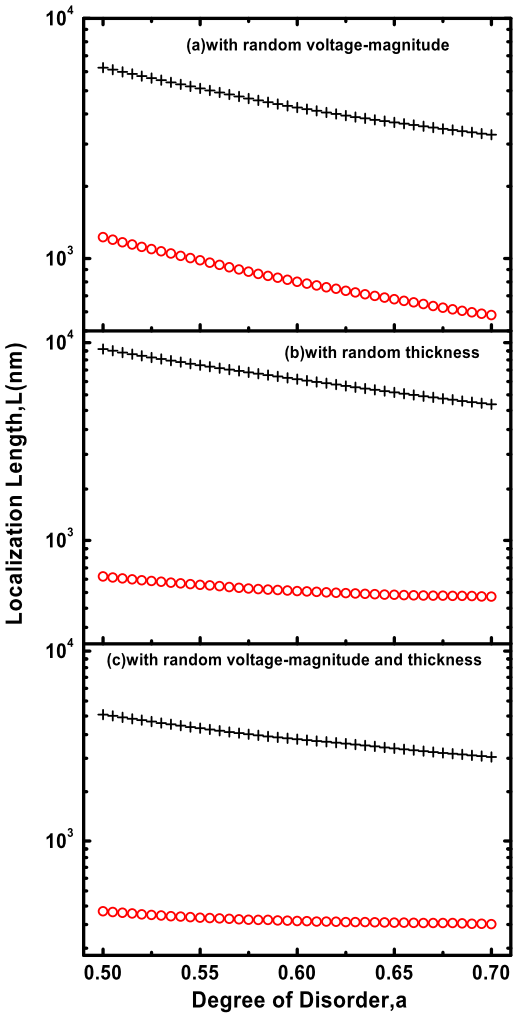

Fig. 9. The localization lengths of $(AB)_{30}$ structures over 1000 configurations in three random cases at the interval $0.5 \leqslant a \leqslant 0.7$ for $E = 10$ meV (the cross scatters) and $E = 83$ meV (the open circular scatters), respectively. The other parameters are the same with those used in Fig. 8.

ture with LH layers are more robust against the disorder than those in the structure with pure RH layers. This confirms that the compensation effect of LH medium occurs no matter what the disorder configuration is. When we further increase the value of a, the average DOS will change too rapidly as the energy varies. Therefore, for $a > 0.5$, we calculate the spectra of localization length l of the random structure that is defined by [2]

$$l^{-1} = \lim_{L\to\infty} \frac{-\langle \ln|t(L)|\rangle}{L}, \tag{4}$$

where L is the sample length and $t(L)$ is the transmission coefficient of the sample. In the limit of infinite L, Eq. (4) gives a well-defined value of l by self-averaging. For a finite, but sufficient large L, l can be obtained from the average of t over many different disorder configurations. In the following calculations, we use 1000 disorder configurations to ensure reliable results. In Fig. 8 we plot the spectra of localization length when the value of a changes from 0.5 to 0.7 in three cases. In the case in which only the voltage-magnitude is random, with the increase of a, the value of l corresponding to the energy bands in Fig. 2(a) will decrease, as is shown in Fig. 8(a). In contrast, the value of l corresponding to the energy gaps in Fig. 2(a) will decrease as the value of a increases. In the case in which thickness fluctuation is involved, the dependence of l on a becomes complex. Note that in the energy band with $90 < E < 95$ meV, the value of l will increase rather than decrease as the value of a increases, as is shown in Fig. 8(b). In all cases, for a fixed value of a, the value of l in $0 < E < 10$ meV is always larger than that in $75 < E < 95$ meV. In Fig. 9 we show the variances of l at two different incident energies when the value of a gradually increases from 0.5 to 0.7. The cross scatters in Fig. 9 correspond to the incident energy $E = 10$ meV and the open circular scatters correspond to $E = 83$ meV. From Fig. 9 one can see that, for both $E = 10$ meV and $E = 83$ meV, at a fixed value of a, the value of l in the case involving both voltage-magnitude and thickness is smallest. Moreover, for the same value of a, the l at $E = 10$ meV is always much longer than that at $E = 83$ meV in all cases. This confirms that Anderson localization is suppressed in the mixed structure with LH and RH layers, compared to the structure with pure RH layers. To summarize, all the spectra of (average) DOS and localization length in three random cases demonstrate that the phase compensation effect of LH layers can reduce the long-range interferences in a disordered electronic structure and suppress Anderson localization.

3. Conclusion

In conclusion, Anderson localization in a graphene sheet with a random voltage pattern in which the magnitudes and/or the

widths of the voltages are random is theoretically studied. A graphene sheet applied by tunable external voltages provides us a convenient platform to study various disordered structures. In particular, when the magnitudes of voltages exceed the electronic energy, LH graphene layers are formed. Similar to the classical counterparts, the LH graphene layers in random electronic structures can compensate the phase accumulations in the RH layers, reduce the long-range interference and suppress Anderson localization.

Acknowledgements

This work was funded by the National Basic Research Program of China (grant 2011CB922001), from the National Natural Science Foundation of China (grants 11074187 and 51007064), from the Program of the Shanghai Science and Technology Committee (grants 08dj1400301 and 11QA1406900), and from the Fundamental Research Funds for the Central Universities.

References

[1] P.W. Anderson, Phys. Rev. 109 (1958) 1492.
[2] I.M. Lifshitz, S.A. Gredeskul, L.A. Pastur, Introduction to the Theory of Disordered System, Wiley, New York, 1989.
[3] S. John, Phys. Rev. Lett. 53 (1984) 2169.
[4] P. Sheng, Scattering and Localization of Classical Waves in Random Media, World Scientific, Singapore, 1991.
[5] V.D. Freilikher, S.A. Gredeskul, in: E. Wolf (Ed.), Progress in Optics, vol. XXX, Elsevier Science, Amsterdam, 1992, Chap. III, p. 137.
[6] V.G. Veselago, Sov. Phys. Usp. 10 (1968) 509.
[7] V.M. Agranovich, Yu.N. Gartstein, Phys. Usp. 49 (2006) 1029.
[8] J. Li, L. Zhou, C.T. Chan, P. Sheng, Phys. Rev. Lett. 90 (2003) 083901.
[9] A.A. Asatryan, L.C. Botten, M.A. Byrne, V.D. Freilikher, S.A. Gredeskul, I.V. Shadrivov, R.C. Mcphedran, Y.S. Kivshar, Phys. Rev. Lett. 99 (2007) 193902.
[10] A.A. Asatryan, S.A. Gredeskul, L.C. Botten, M.A. Byrne, V.D. Freilikher, I.V. Shadrivov, R.C. McPhedran, Y.S. Kivshar, Phys. Rev. B 81 (2010) 075124.
[11] A.A. Asatryan, L.C. Botten, M.A. Byrne, V.D. Freilikher, S.A. Gredeskul, I.V. Shadrivov, R.C. McPhedran, Y.S. Kivshar, Phys. Rev. B 82 (2010) 205124.
[12] V. Baluni, J. Willemsen, Phys. Rev. A 31 (1985) 3358.
[13] D. Mogilevtsev, F.A. Pinheiro, R.R. dos Santos, S.B. Cavalcanti, L.E. Oliveira, Phys. Rev. B 82 (2010) 081105.
[14] Y. Dong, X. Zhang, Phys. Lett. A 359 (2006) 542.
[15] E.M. Nascimento, F.A.B.F. de Moura, M.L. Lyra, Opt. Express 16 (2008) 6860.
[16] K.S. Novoselov, A.K. Geim, S.V. Morozov, D. Jiang, Y. Zhang, S.V. Dubonos, I.V. Grigorieva, A.A. Firsov, Science 306 (2004) 666.
[17] Y. Zhang, Y.W. Tan, H.L. Stormer, P. Kim, Nature (London) 438 (2005) 201.
[18] C.W.J. Beenakker, Rev. Mod. Phys. 80 (2008) 1337;
A.H. Castro Neto, F. Guinea, N.M.R. Peres, K.S. Novoselov, A.K. Geim, Rev. Mod. Phys. 81 (2009) 109.
[19] V.V. Cheianov, V. Fal'ko, B.L. Altshuler, Science 315 (2007) 1252.
[20] L.G. Wang, S.Y. Zhu, Phys. Rev. B 81 (2010) 205444.
[21] H.T. Jiang, Z.L. Wang, Z.G. Wang, H. Chen, Phys. Lett. A 375 (2011) 1014.
[22] J.M. Bendickson, J.P. Dowling, M. Scalora, Phys. Rev. E 53 (1996) 4107.
[23] S.F. Liew, H. Cao, J. Opt. 12 (2010) 024011.